ECS Solid State Letters, **2** (2) P15-P18 (2013)
2162-8742/2013/2(2)/P15/4/$28.00 © The Electrochemical Society

Concentration Gradient of Ni in Reduced SnAg Thickness in Ni/SnAg/Cu Microbumps during Solid-State Aging

Tao-Chi Liu, Yi-Sa Huang, and Chih Chen[z]

Department of Materials Science & Engineering, National Chiao Tung University, Hsin-chu 30010, Taiwan

We investigate the cross-interaction in Cu/SnAg/Ni microbumps with a reduced solder thickness of 30 and 10 μm. The concentration of Ni atoms at the opposite site increased with the decrease in solder-height. A considerable concentration gradient of Ni was detected in 10-μm microbumps sample, which strongly triggers the diffusion of Ni atoms to the Cu side. The diffused Ni atoms at Cu side form the ternary intermetallic compounds of $(Cu,Ni)_6Sn_5$, which possesses a lower free energy than Cu_6Sn_5 does. Eventually, the growth of the Cu_3Sn was inhibited due to the formation of the thermodynamically stable $(Cu,Ni)_6Sn_5$.
 [DOI: 10.1149/2.009302ssl]

Manuscript submitted July 16, 2012; revised manuscript received November 7, 2012. Published November 28, 2012.

Three-dimension (3D) integrated circuits (ICs) packaging offers a high system integration by connecting multiple ICs chips which have different functions. To minimize the vertical packaging size, microbumps are adopted for connecting the I/O pads on between chips.[1–4] The bump height of the microbump is typical between 5 to 20 μm and the solder volume is smaller than traditional solder bumps. The distance between the two metallization pads across the solder is very close as well.

During the reflow processes, solder reacts with the metallization materials, to form the intermetallic compounds (IMCs). Two chips are joined together through the IMCs in the microbumps. When two different metallization materials are adopted across the solder joints, interdiffusion can occur inside the solder joints during reflow process or solid-state aging.[5–7] For example, it is quite common that Cu is adopted as one of the metallization material, and Ni serves the other one on the opposite side. Cu atoms may diffuse to the Ni side to affect the growth of the interfacial IMCs. Ni atoms can also migrate to the Cu end to influence the IMCs there.[8–12] Furthermore, the minor species in solder can also affect the growth of interfacial IMCs.[13–21] For instance, a small amount of Ni in solder is able to influence the growth of microstructure in the Cu_6Sn_5 IMCs.[22–25] It is reported that the addition of Ni atoms will ease the formation of Cu_3Sn.[26,27]

During solid-state aging, Chang et al.[9] found that the atomic flux of Ni is about 25-40 times lower than that of Cu in ball grid array (BGA) and flip chip packaging. Nevertheless, Ni atoms still diffused through 400 μm solder and affected the interfacial reaction on the other side after several hundred hours of thermal aging. As the bump height continuous to shrink in 3D IC packaging, the interdiffusion between the two metallization materials become more significant, but only few studies discussed the issue. Huang et al.[28] reported a Ni concentration gradient in reflowed microbumps dominated the IMCs thickness during reflow process. However, whether there exists a Ni concentration gradient during solid-state aging and the Ni distribution in the Cu-Ni-Sn ternary IMCs are not clear. However, the concentration of Ni across the low-bump-height solder joint and its effect on the IMCs growth have not been reported. In this study, we investigate the cross-interaction across the solder joints with two different bump heights. A detailed focused ion beam (FIB) study including cross-sectional polishing and morphologies observation of $(Cu,Ni)_6Sn_5$ and Cu_3Sn IMCs has been performed. Compositional analysis by electron probe X-ray microanalyzer (EPMA) was performed to map the distribution of Cu and Ni atoms in the microbumps.

Experimental

To prepare the microbumps, materials for under bump metallurgy (UBM) were firstly deposited on a Si substrate by electroplating a metal layer of 3-μm Ni or 10-μm Cu, and then followed by the electroplating of Sn2.3Ag lead-free solder on the Ni or Cu UBM. A chip with Cu/Sn2.3Ag microbumps was flipped over and joined to another chip with Ni/Sn2.3Ag microbumps at 260°C for 3 min on a hot plate. Thus, Cu/Sn2.3Ag/Ni sandwich samples can be fabricated. Similarly, controlled samples of Cu/Sn2.3Ag/Cu structure were prepared by bonding two chips with Cu/Sn microbumps. The solder height was controlled to a thickness of approximately 10 μm and 30 μm in the bonded microbumps. Then solid-state aging was performed at 150°C for 0, 100, 500 and 1000 h in a nitrogen-filled oven. To clearly observe the morphologies of IMCs, the aged samples were cross-sectioned and were polished utilizing a dual-beam FIB. The details for the polishing procedure is reported in our previous publication.[29] Therefore, the microstructure of the thin Cu_3Sn and $(Cu,Ni)_6Sn_5$ can be observed without suffering mechanical destruction. Elemental distributions were analyzed by FE-EPMA (JXA-8800M, JEOL).

Results and Discussion

With the FIB polishing, different layers exhibit clear contrasts in FIB images, as shown in Figures 1. Figure 1a shows the cross-sectional FIB image for an as-fabricated microbump. The $(Cu,Ni)_6Sn_5$ IMCs form in both the solder/Ni and solder/Cu interfaces with 10-μm-thick solder. The IMCs thickness on the Cu side was thicker than that on the Ni side, which has been reported by Huang et al.[28] A thin Cu_3Sn layer formed between the $(Cu,Ni)_6Sn_5$ and Cu UBM, as labeled in the Figure. Compositional analysis by EPMA indicates that the Ni concentration is 0.7 at.% in the solder close to the $(Cu,Ni)_6Sn_5$ IMC on the Cu side. Yet, it is 1.3 at.% in the solder near to the

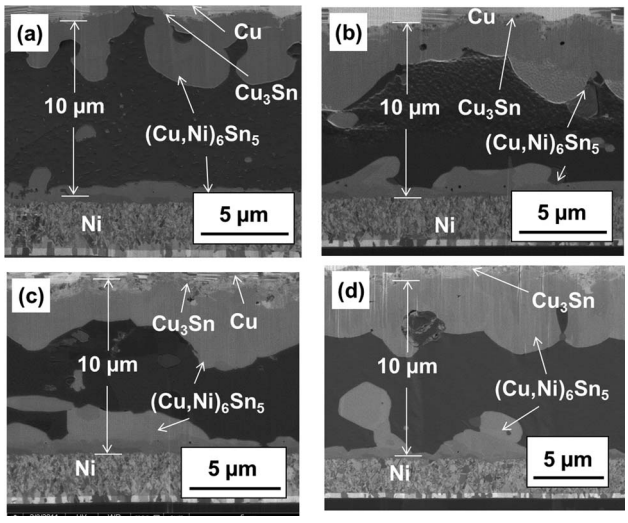

Figure 1. Cross-sectional FIB image for (a) the as-fabricated Cu/Sn2.3Ag/Ni microbump reflowed at 240°C after 3 min; and solid-state aged at 150°C for (b)100 h; (c) 500 h; (d) 1000 h.

[z]E-mail: chih@mail.nctu.edu.tw

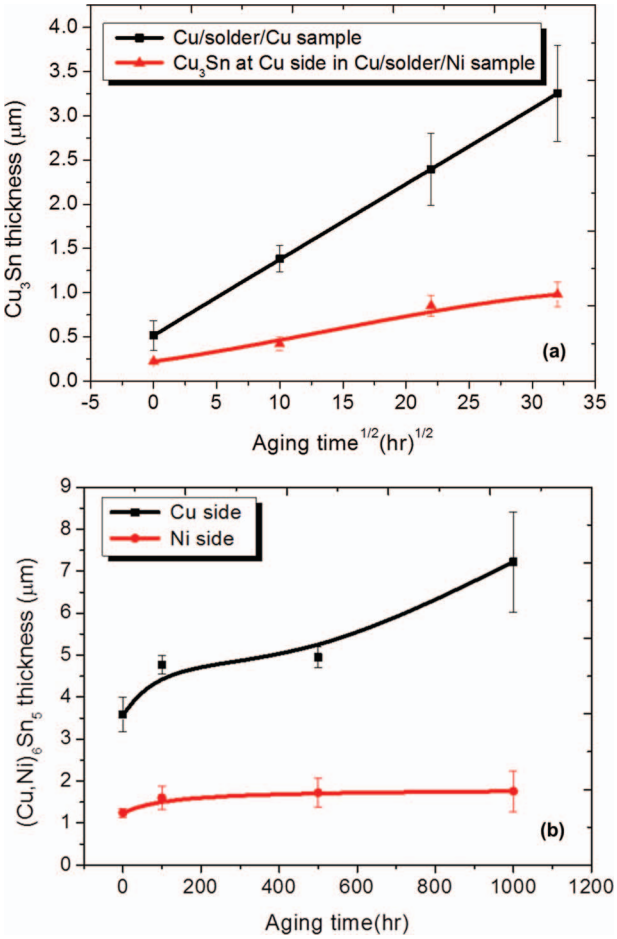

Figure 2. (a) The measured thickness of Cu_3Sn IMCs at 150°C against the square root of the aging time for Cu/Sn2.3Ag/Ni and Cu/Sn2.3Ag/Cu microbumps. (b) The average thickness of (Cu, Ni)$_6Sn_5$ on the Cu and Ni sides as a function of the aging time for Cu/Sn2.3Ag/Ni microbumps.

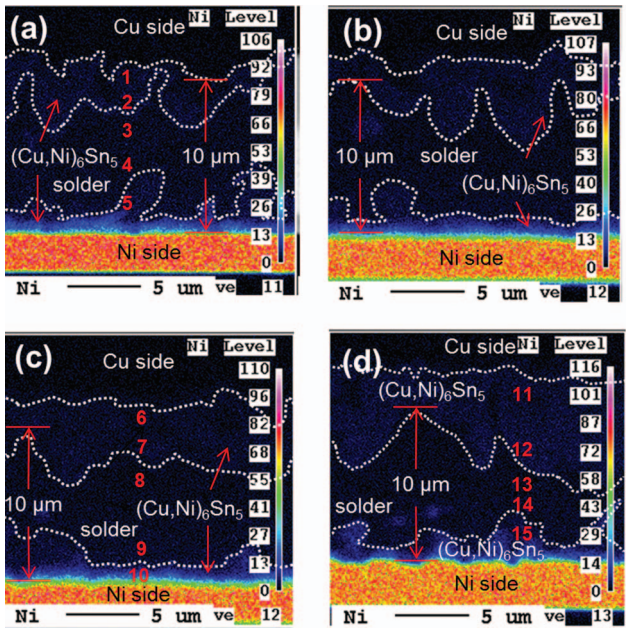

Figure 3. EPMA color mapping of Cu/Sn2.3Ag/Ni microbumps aged at 150°C showing Ni distributions for (a) 0 h; (b) 100 h; (c)500 h and (d) 1000 h.

(Cu,Ni)$_6Sn_5$ IMCs on the Ni side. Thus, there exists a Ni concentration gradient across the solder joint during solids-state aging at 150°C, which provides the driving force for the Ni to diffuse to the Cu side. In addition, it is reported that the formation of ternary Cu-Ni-Sn IMCs will lower the free energy of the system.[30,31] Thus, the change of the free energy also drives the diffusion of the Ni atoms to the Cu side.

The Ni UBM can effectively inhibit the growth of the Cu_3Sn IMCs at the Cu side. Figure 1b to 1d present the cross-sectional FIB images for the Cu/Sn2.3Ag/Ni sample after aging at 150°C for 100,500, and 1000 h, respectively. The IMCs on the both interfaces grew thicker when the aging time increased. In particular, the (Cu,Ni)$_6Sn_5$ IMCs on the Cu side grew from 3.8 μm to 7.2 μm after the aging for 1000 h. However, it is interesting that the Cu_3Sn layer did not grow much. The thickness of the Cu_3Sn was only 1.0 μm after 1000 h aging. For comparison, the controlled sample of Cu/Sn2.3Ag/Cu was also aged at 150°C for 1000 h. Figure 2a shows the measured Cu_3Sn thickness as the square root of the aging time for both samples. It is apparent that the Cu_3Sn IMCs in the Cu/Sn2.3Ag/Cu grew faster than that in the Cu side of the Cu/Sn2.3Ag/Ni sample. The Cu_3Sn layer can grow to 3.2 μm after aging for 1000 h in Cu/SnAg/Cu sample. Figure 2b illustrates the thickness of (Cu,Ni)$_6Sn_5$ IMCs against the aging time in the Cu/Sn2.3Ag/Ni sample. The IMCs on the Cu side grew much faster than that on the Ni side. Yet, the Cu_3Sn layer grew to only 1.0 μm after 1000 h aging. Therefore, it is evident that the Ni UBM can ease the growth of the Cu_3Sn layer on the Cu side, although the (Cu,Ni)$_6Sn_5$ on the Cu side has grown to 7.2 μm.

To examine how the Ni atoms can ease the growth of the Cu_3Sn, elemental mapping of Cu and Ni atoms was carried out by EPMA. Figure 3a through 3d shows the evolution of Ni distributions in the microbumps after aging for 0, 100, 500, and 1000 h. In addition, quantitative analysis was also performed to measure the concentration of Cu, Ni, Ag and Sn in the samples at various locations. Table I lists the measured concentrations for the four elements. The results show that Ni atoms diffused to the Cu side to form (Cu,Ni)$_6Sn_5$ IMCs. The Ni atoms dissolved in the IMCs relatively uniformly. In addition, as the aging time increased, not only the IMCs on Cu side became thicker, but also the Ni concentration in the IMCs increased. The Ni concentration was 2.0 at.% in the (Cu,Ni)$_6Sn_5$ close to the solder. It increased to 2.4 at.% after the aging for 500 h and 1000 h. The trend behaves the same in the (Cu,Ni)$_6Sn_5$ IMCs close to the Cu_3Sn layer. Therefore, a lot of Ni atoms diffused to the Cu side during the solid state aging. The formation of the (Cu,Ni)$_6Sn_5$ IMCs may inhibit the growth of Cu_3Sn layer on the Cu side due to the (Cu,Ni)$_6Sn_5$ IMCs possess a lower free energy than Cu_6Sn_5 does.[28,29] During solid-state aging, Cu_3Sn IMCs grows at the expense of Cu_6Sn_5.[32] Therefore, the Cu_3Sn layer grow slowly when the Cu_6Sn_5 IMCs transform into (Cu,Ni)$_6Sn_5$ IMCs, which has a lower free energy than Cu_6Sn_5.

The EPMA results indicate that a Ni concentration gradient across the solder joints is increased with the decrease in solder-height. Figure 4a and 4b show the cross-sectional SEM image of the 10-μm and 30-μm solder, respectively. The numbers labeled on the figures represent the locations for EPMA compositional analysis. Table II lists the Ni concentrations of the three locations and the corresponding concentration gradient of Ni across the solder joint. The average Ni concentration is 2.3 ± 0.3 at.% and 0.9 ± 0.2 at.% in (Cu,Ni)$_6Sn_5$ IMCs on the Cu side of the 10-μm and 30-μm solder, respectively. Furthermore, in 10-μm solder sample, both the concentration of Ni in solder and the concentration gradient of Ni are higher than those in the 30-μm solder sample. For 30-μm solder sample, the Cu side (Cu,Ni)$_6Sn_5$ IMCs and Cu_3Sn grew to 7.4 μm and 2.8 μm, respectively. It is evident that the Ni flux to the Cu side in the 10-μm solder sample is higher than that in the 30-μm solder sample, which may be mainly attributed to the higher Ni concentration gradient in the 10-μm solder sample. As mention earlier, the thickness of Cu_3Sn IMCs in 10-μm solder sample is only 1.0 μm. The higher Ni flux eliminates the Cu_3Sn effectively.

Table I. Result of compositional analysis by EPMA (beam size 0.5 μm) at different locations in the Cu/Sn2.3Ag/Ni microbumps.

			Atomic percentage (%)			
Aging	Point	Location	Sn	Ag	Cu	Ni
0 h	1	$(Cu,Ni)_6Sn_5$ close to Cu_3Sn on Cu side	25.0	< 0.1	74.5	0.4
	2	$(Cu,Ni)_6Sn_5$ close to solder on Cu side	44.5	0.2	53.3	2.0
	3	Solder near Cu side	95.5	< 0.1	3.8	0.7
	4	Solder near Ni side	95.7	< 0.1	2.9	1.3
	5	$(Cu,Ni)_6Sn_5$ at Ni side	45.0	0.1	50.6	4.3
500 h	6	$(Cu,Ni)_6Sn_5$ close to Cu_3Sn on Cu side	25.0	< 0.1	74.4	0.6
	7	$(Cu,Ni)_6Sn_5$ close to solder on Cu side	46.8	< 0.1	50.7	2.4
	8	Solder near Cu side	96.2	< 0.1	3.2	0.6
	9	Solder near Ni side	95.5	< 0.1	2.4	2.1
	10	$(Cu,Ni)_6Sn_5$ at Ni side	45.1	< 0.1	30.5	24.4
1000 h	11	$(Cu,Ni)_6Sn_5$ close to Cu_3Sn on Cu side	26.2	< 0.1	72.6	1.1
	12	$(Cu,Ni)_6Sn_5$ close to solder on Cu side	45.8	< 0.1	51.6	2.4
	13	Solder near Cu side	95.8	< 0.1	3.8	0.5
	14	Solder near Ni side	95.8	< 0.1	2.6	1.7
	15	$(Cu,Ni)_6Sn_5$ at Ni side	40.8	< 0.1	26.9	32.3

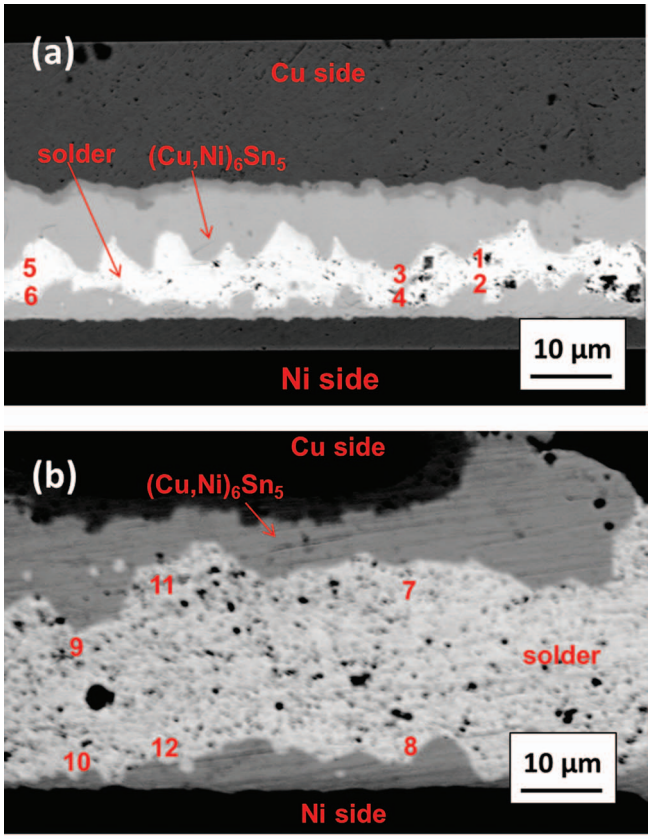

Figure 4. Cross-sectional SEM image showing the locations of EPMA quantitative analysis for the Cu/Sn2.3Ag/Ni microbumps with a bump-height of (a) 10 μm and (b) 30 μm, aged at 150°C for 1000 h.

Table II. Result of compositional analysis by EPMA at different locations in the Cu/Sn2.3Ag/Ni microbumps in Figure 4.

Bump height	Point	Ni at.%	Solder length between the measured points(μm)	Concentration gradient (at.% per μm)
	1	0.3	5.1	0.24
	2	1.5		
	3	0.5	2.9	0.31
10 μm	4	1.4		
	5	0.9	10.0	0.04
	6	1.3		
	7	0.7	27.8	0.01
	8	0.9		
30 μm	9	0.8	17.8	0.01
	10	0.7		
	11	0.8	24.4	0.00
	12	0.7		

Conclusions

In summary, we have examined the cross-interactions in the Ni/Sn2.3Ag/Cu in the 10-μm and 30-μm solder-height microbumps. When the solder-height reduce to 10 μm, it is found that the $(Cu,Ni)_6Sn_5$ IMCs on the Ni side grew slowly during solid state aging at 150°C. However, the $(Cu,Ni)_6Sn_5$ IMCs on the Cu side grew faster than those on the Ni side. The formation of the ternary $(Cu,Ni)_6Sn_5$ on the Cu side suppress the growth of Cu_3Sn IMCs due to the lower free energy of the ternary IMCs. EPMA quantitative analysis demonstrated that the Ni concentration gradient of the microbumps plays an important role to the Ni diffusion during solid-state aging.

Acknowledgment

The authors gratefully acknowledge the financial support by the National Science Council of the Republic of China (Grant No. NSC 98-2221-E-009-036-MY3).

References

1. Robert S. Patti, *Proceedings of the IEEE*, **94**(6), 1215 (2006).
2. H. Y. You, Y. S. Lee, S. K. Lee, and J. S. Kang, in *61th Electronic Components & Technology Conference*, 608 (2011).
3. T. H. Lin, R. D. Wang, M. F. Chen, C. C. Chiu, S. Y. Chen, T. C. Yeh, Larry C. Lin, S. Y. Hou, J. C. Lin, K. H. Chen, S. P Jeng, and Douglas C. H. Yu, in *61th Electronic Components & Technology Conference*, 346 (2011).
4. C. C. Wei, C. H. Yu, C. H. Tung, R. Y. Huang, C. C. Hsieh, C. C. Chiu, H. Y. Hsiao, Y. W. Chang, C. K. Lin, Y. C. Liang, C. Chen, T. C. Yeh, Larry C. Lin, and Doug C. H. Yu, in *61th Electronic Components & Technology Conference*, 706 (2011).
5. C. H. Yu and K. L. Lin, *J. Mater. Res.*, **20**(3), 666 (2005).
6. T. Sasaki, M. Tanaka, and Y. Ohno, *Mater. Lett.*, **61**, 2093 (2007).
7. H. W. Tseng and C. Y. Liu, *Mater. Lett.*, **2**, 3887 (2008).
8. S. J. Wang and C. Y. Liu, *Scripta. Mater.*, **55**, 347 (2006).
9. C. W. Chang, S. C. Yang, C. T. Tu, and C. R. Kao, *J. Electron. Mater.*, **36**, 1455 (2007).
10. K. K. Hong, J. B. Ryu, C. Y. Park, and J. Y. Huh, *J. Electron. Mater.*, **37**(1), 61 (2008).
11. W. H. Wu, H. L. Chung, C. N. Chen, and C. E. Ho, *J. Electron. Mater.*, **38**(12), 2563 (2009).
12. T. L. Shao, T. S. Chen, Y. M. Huang, and C. Chen, *J. Mater. Res.*, **19**(12), 3654 (2004).

13. C. Y. Yu and J. G. Duh, *Scripta Mater.*, **65**, 783 (2011).
14. J. Y. Kim, J. Yu, and S. H. Kim, *Acta Mater.*, **57**, 5001 (2009).
15. K. Zeng and K. N. Tu, *Mater. Sci. Eng.*, **38**, 55 (2002).
16. J. Y. Kim and J. Yu, *Appl. Phys. Lett.*, **92**, 092109 (2008).
17. C. H. Wang and H. T Shen, *Intermetallics*, **18**, 616 (2010).
18. P. J. Shang, Z. Q. Liu, D. X. Lia, and J. K. Shang, *Scripta Mater.*, **58**, 409 (2008).
19. Y. Lee and M. Li, *Metall. Trans. A*, **32A**, 2666 (2001).
20. P. T. Vianco, J. J Martin, R. D. Wright, and P. F. Hlava, *Metall. Trans. A*, **38A**, 2488 (2007).
21. T. C. Chang, M. H. Hon, and M. C. Wang, *Electrochemical and Solid-State Letters*, **7**(2), J4 (2004).
22. C. Y. Yu, T. K. Lee, M. Tsai, K. C. Liu, and J. G Duh, *J. Electron Mater.*, **39**, 2544 (2010).
23. J. Y. Tsai, Y. C. Hu, C. M. Tsai, and C. R. Kao, *J. Electron Mater.*, **32**, 1203 (2003).
24. T. Ventura, S. Terzi, M. Rappaz, and A. K. Dahle, *Acta Mater.*, **59**, 4197 (2001).
25. C. Y. Liu, H. W. Tseng, and J. M. Song, *Electrochemical and Solid-State Letters*, **13**(9), H298 (2010).
26. Y. W. Wang, Y. W. Lin, and C. R. Kao, *Microelectron. Reliab.*, **49**, 248 (2009).
27. Y. W. Wang, C. C. Chang, W. M. Chen, and C. R. Kao, *J. Electron Mater.*, **39**(12), 2636 (2010).
28. Y. S. Huang, H. Y. Hsiao, C. Chen, and K. N. Tu, *Scripta Mater.*, **66**, 741 (2012).
29. Tao-Chi Liu, Chih Chen, Kuo-Jung Chiu, Han-Wen Lin, and Jui-Chao Kuo, *Materials Characterization*, **74**, 42 (2012).
30. C. Yu, J. Liu, H. Lu, P. Li, and J. Chen, *Intermetallics*, **15**, 1471 (2007).
31. K. Nogita and T. Nishimura, *Scripta Mater.*, **59**, 191 (2008).
32. K. N. Tu, *Solder Joint technology materials, properties, and reliability*, p. 58, Springer Science, New York (2007).